FARADAY

Mixed crystals of *n*-alkane pairs

A global view of the thermodynamic melting properties

D. Mondieig,[a]* P. Espeau,[a] L. Robles,[a] Y. Haget,[a] H. A. J. Oonk[b] and M. A. Cuevas-Diarte[c]

[a] *Centre de Physique Moléculaire Optique et Hertzienne,† UMR au CNRS, Université Bordeaux I, 351 Cours de la Libération, 33405 Talence, France*

[b] *Department of Interfaces and Thermodynamics,† Faculty of Chemistry and Petrology Group, Faculty of Earth Sciences, Utrecht University, Budapestlaan 4, 3584 CD Utrecht, The Netherlands*

[c] *Department de Cristallografia,† Mineralogia i Diposits Minerals, Universitat de Barcelona, Marti i Franques, s/n, 08028 Barcelona, Spain*

The excess thermodynamic melting properties of the mixed crystalline rotator form of binary mixtures of neighbours and next-nearest neighbours of *n*-alkanes in the range $C_{11}H_{24}$ to $C_{26}H_{54}$ are characterized by a uniform temperature of enthalpy/entropy compensation of 320 K. Excess enthalpy differences have been obtained by microcalorimetry and excess Gibbs energy differences by phase diagram analysis and the two properties were combined to give the excess entropy differences. The excess enthalpy and excess entropy differences are negative and their absolute values, which are virtually equal to the excess properties of the rotator form, increase with increasing relative mismatch between the crystallographic unit cells of the two components involved.

Introduction

In recent years a considerable amount of work has been carried out on the structural and thermodynamic characteristics of binary and ternary systems of *n*-alkanes as well as on their suitability as phase change materials for the storage of thermal energy.[1–21]

The systems dealt with in this paper are binary systems in which the two components are either neighbours or next-nearest neighbours in the range from $C_{11}H_{24}$ to $C_{26}H_{54}$. The detailed results obtained for these systems have been laid down in the theses, presented at the University of Bordeaux I, by P. Espeau[1] (range $C_{11}H_{24}$–$C_{17}H_{36}$) and L. Roblès[2] (range $C_{18}H_{38}$–$C_{26}H_{54}$).

n-Alkanes (C_nH_{2n+2}, abbreviated in this paper to C_n) have a polymorphic nature.[1,2,22–32] In the range of interest of this paper, which is the range in which the transition from solid to liquid takes place, three different forms can be recognized. These are the triclinic form (T) and two so-called rotator forms (RI and RII).

RI and RII are rotator phases characterized by orientational disorder.[1,2,22–30] In RI the molecules undergo large oscillations around their long axes. In RII the molecules show complete rotation around their long axis. When observed, the transition from RI to RII is first-order, the energy effect involved being very small (typically $\leqslant$0.4 kJ mol^{-1}). From a structural point of view RI and RII are very similar.

The crystallographic characteristics of the forms are as follows: form T has space group $P\bar{1}$ with $Z = 1$ (1 molecule per unit cell); RI is orthorhombic with space group *Fmmm* and $Z = 4$ and RII is hexagonal with space group $R\bar{3}m$ and $Z = 3$. The *n*-alkanes involved in this paper range from C_{11} to C_{26}. They show the following trends as regards the (stable) form which melts: for $12 \leqslant n \leqslant 20$, where *n* is even, the form that melts is T; for $11 \leqslant n \leqslant 21$, where *n* is odd, the form that melts is RI; for $22 \leqslant n \leqslant 26$, the melting form is RII.

† Member of the REALM (Reseau Européen sur les Alliages Moléculaires) gathers four research groups from four universities [two in Barcelona (Central and Polytechnical), Bordeaux, Utrecht] General coordinator: Y. Haget.

In this paper a concise overview is given of the thermodynamic aspects of the transition from the rotator form (RI and RII) to the liquid. The information which has become available represents a set of thermodynamic mixing data on a chemically coherent group of binary systems. Therefore, the principal question to be answered in this paper is: which relationships, thermodynamic and/or exothermodynamic, emerge from the set of experimental data?

Experimental data

In this section a brief survey is given of the experimental data and the methodology of their determination; for details see ref. 1–7. In all cases microcalorimetry was used to establish the phase diagrams and simultaneously the energetic effects of the various transitions. In most cases X-ray diffraction was used to confirm the calorimetric results.

From the remarks made above, it is obvious that for a number of systems the components do not have the same 'melting forms'. Indeed, the complete phase diagrams can be rather complex; some typical examples of phase diagrams are shown in Fig. 1–4. The figures clearly show that the transition from rotator to liquid extends over a wide range if not all of the composition axis.

For each binary system the enthalpy effects were measured as a function of composition. From these effects and the corresponding pure component effects, the excess enthalpy differences ΔH^E (*i.e.* enthalpy of liquid minus enthalpy of solid) were calculated. In a number of cases this requires knowledge of the metastable melting properties of the pure components; these properties could easily be obtained (correlations as a function of chain length).

By thermodynamic phase diagram analysis the excess Gibbs energy difference ΔG^E was calculated. The method used was LIQFIT,[33] which is a procedure based on the equal-*G* curve concept (see ref. 34).

Finally, by combining ΔG^E and ΔH^E the excess entropy difference ΔS^E was calculated from

$$\Delta G^E(T_m, x) = \Delta H^E(x) - T_m \Delta S^E(x) \quad (1)$$

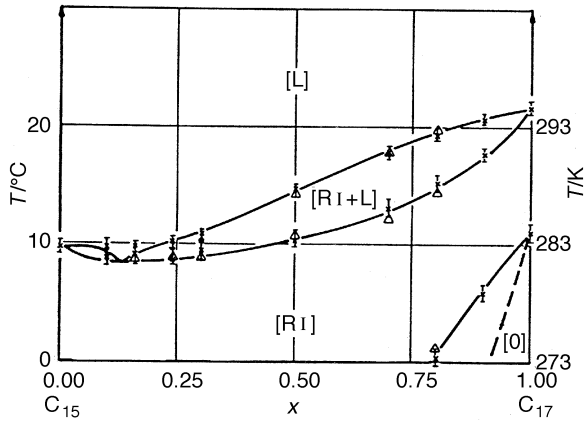

Fig. 1 Phase diagram of C_{15}–C_{17}; (×) data obtained by microcalorimetry, (△) data obtained by X-ray diffraction

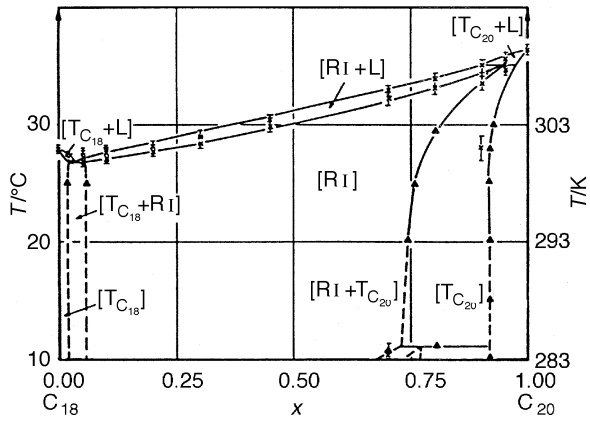

Fig. 3 Phase diagram of C_{18}–C_{20}; [mixing the triclinic forms (T) of the components induces the rotator form (RI)]; (×) data obtained by microcalorimetry, (▲) obtained by X-ray diffraction

where T_m is the mean temperature, for a given system, of the solid-to-liquid transition and x is the mole fraction.

A survey of the experimental data for equimolar compositions is given in Table 1. In the table a code is used as to the solid (rotator) forms involved, as well as regards the thermodynamic nature of the pure components (*i.e.* stable or metastable for the transition taken into account). It may be noted that the difference data in Table 1 have been presented with opposite signs. The reason for this is that, in the case of pairs of substances that give rise to mixed crystals, the deviation from ideality in the liquid state is usually small with respect to the deviation in the solid (mixed crystalline) state, *i.e.* $\Delta H^E = H^E_{liq} - H^E_{sol} \approx H^E_{sol}$. Therefore, one can say that the excess values given in the columns of the table are representative of the solid state.

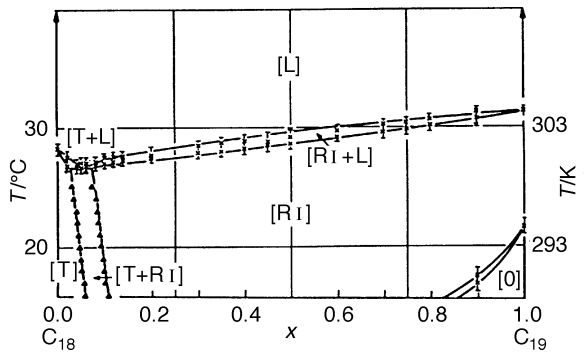

Fig. 2 Phase diagram of C_{18}–C_{19}; (×) data obtained by microcalorimetry, (▲) data obtained by X-ray diffraction

Correlation and Discussion

Doing research on families of systems is extremely rewarding for a number of reasons. From an experimental point of view there is an extra check as regards the consistency of the data. In addition, a phenomenon which has escaped the attention in one system may make a clear appearance in another. Most importantly, families of systems offer the possibility of making correlations between different thermodynamic properties and correlations between thermodynamic properties and non-

Table 1 Survey of experimental information on the thermodynamic excess properties of the transition from rotator solid-to-liquid for the equimolar mixtures. Circles are used to indicate rotator phase RII and ellipses to indicate rotator phase RI. Shading (partial or full) is used for cases where the pure component(s) is (are) not stable in the solid form considered.

system	code	$T_{EGC}(x = 0.5)$/K	$-\Delta H^E(x = 0.5)$/J mol^{-1}	$-\Delta G^E(x = 0.5)$/J mol^{-1}	$-\Delta S^E(x = 0.5)$/J K^{-1} mol^{-1}
$\Delta n = 1$					
C_{23}–C_{24}	⊖	322.2	850	−50	2.8
C_{22}–C_{23}	⊖	318.5	850	−50	2.8
C_{19}–C_{20}	◒	306.6	1000	0	3.3
C_{18}–C_{19}	◐	301.8	900	50	2.8
C_{17}–C_{18}	◒	299.6	1300	80	4.0
C_{15}–C_{16}	◒	284.3	1100	135	3.4
C_{14}–C_{15}	◒	277.2	1350	190	4.2
C_{13}–C_{14}	◒	269.8	1210	215	3.7
C_{12}–C_{13}	◒	260.4	1400	245	4.4
C_{11}–C_{12}	◒	250.0	1600	265	5.3
$\Delta n = 2$					
C_{24}–C_{26}	⊖	326.5	1270	−50	4.0
C_{23}–C_{25}	⊖	323.5	2000	−50	6.3
C_{22}–C_{24}	⊖	319.7	1800	60	5.4
C_{20}–C_{22}	◐	312.5	2100	100	6.4
C_{18}–C_{20}	●	303.5	2800	125	8.8
C_{17}–C_{19}	⊖	297.9	2450	250	7.4
C_{15}–C_{17}	⊖	285.6	3250	380	10.0
C_{14}–C_{16}	●	277.8	2600	435	7.8
C_{13}–C_{15}	⊖	270.7	3700	480	11.9

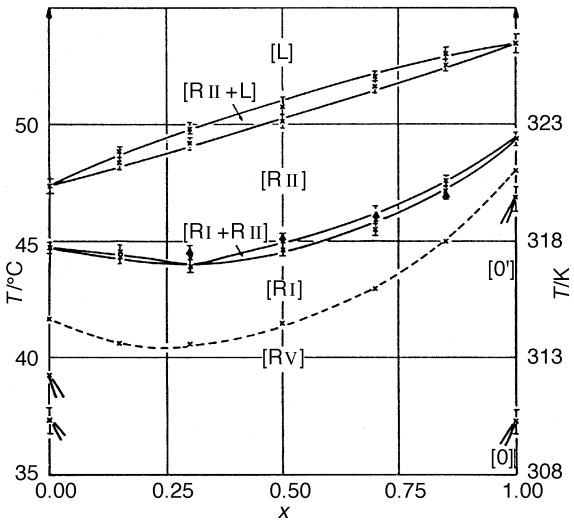

Fig. 4 Phase diagram of C_{23}–C_{25} showing complete miscibility in either of the two rotator forms RI and RII. The dashed curve represents the second-order transition from the rotator phase RV to RI. (×) Data obtained by microcalorimetry, (▲) data obtained by X-ray diffraction.

thermodynamic parameters. Frequently such correlations have far-reaching consequences. For these reasons, the research groups participating in REALM focus their research on families of systems rather than on an equally great number of isolated systems.

In many cases enthalpy differences and entropy differences are virtually constant over a considerable range of temperatures. In such a case the Gibbs energy difference varies in a linear manner with temperature, because of

$$\Delta G = \Delta H - T\Delta S \tag{2}$$

Moreover, ΔH and ΔS often have the same sign as a result of which they 'compensate' one another. This is to say that there is a temperature, θ, for which the excess Gibbs energy goes through zero; θ therefore follows from

$$\theta = \frac{\Delta H}{\Delta S} \tag{3}$$

As an example, the melting point of a pure substance is the temperature at which the enthalpy of melting and the entropy of melting compensate one another.

In the case of the families of systems studied, the excess differences, ΔH^E and ΔS^E, invariably have the same sign. As a result there is, for each of the systems, a compensation temperature for the excess property. Surprisingly, over the whole family, these compensation temperatures are virtually the same. This is demonstrated by Fig. 5 in which the equimolar excess enthalpy differences are plotted against the equimolar excess entropy differences. The important observation which can be made is that the rotator solid-to-liquid transition of the *n*-alkane family is characterized by a single value of 320 K as the compensation temperature for thermodynamic excess properties; *i.e.* the *n*-alkane family represents a class of similar systems having a system independent compensation temperature (see ref. 35).

An interesting relationship is obtained when the excess Gibbs energy difference values (Table 1) are plotted against chain length (the chain length of the smaller component is taken); see Fig. 6. First of all, there are two series, *i.e.* one for $\Delta n = 2$ and the other for $\Delta n = 1$. One can observe that for a given value of n the ΔG^E values for $\Delta n = 2$ are about twice the values for $\Delta n = 1$. The fact that the ΔG^E values become less and less negative and go through zero for about $n = 22$, is the combined result of two factors. These factors are the increase of melting temperature with chain length (which follows

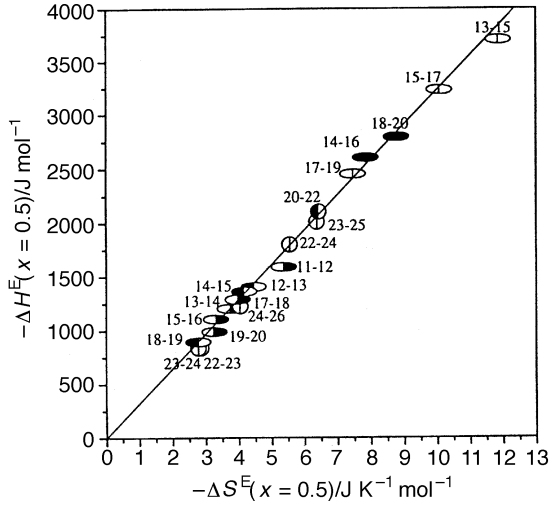

Fig. 5 Representation of excess enthalpy difference as a function of excess entropy difference showing that the *n*-alkane family has a characteristic compensation temperature of 320 K

clearly from Fig. 1 to 4) and the excess enthalpy–entropy compensation at 320 K. In the case of the system C_{15}–C_{17} the melting region is well below 320 K; the ΔG^E value given in Table 1 is valid for 285.6 K. The negative ΔG^E gives rise to a phase diagram with a minimum. In the case of the system C_{23}–C_{25}, 320 K lies within the melting region. At $x = 0.5$ the ΔG^E is slightly positive; the solid–liquid loop has, on average, a somewhat concave appearance.

In contrast to ΔG^E, the excess enthalpy difference, ΔH^E, is virtually independent of temperature (from theoretical considerations it follows that the excess Gibbs energy from 0 K at first displays a rather complex nature, after which it changes in a more or less linear manner with temperature, which results from a constant excess entropy and, also therefore, a constant excess enthalpy, see *e.g.* ref. 36). For that reason the experimental ΔH^E values are more suitable as a basis for an exothermodynamic relationship. An excellent parameter for such a relationship is the coefficient of crystalline isomorphism which quantifies the geometric mismatch between the crystallographic unit cells of the two pure components of a binary system.[37,38] The coefficient is defined as:

$$\varepsilon^i_m = 1 - \Delta_m/\Gamma_m \tag{4}$$

where Δ_m is the excluded and Γ_m the common volume when the two isomorphous unit cells are brought to maximum

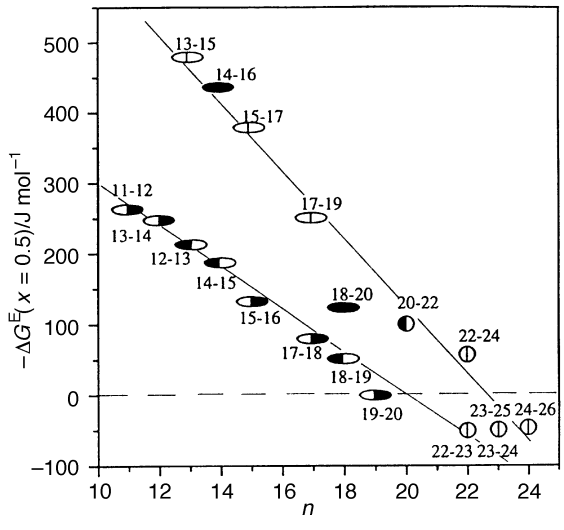

Fig. 6 Plot of excess Gibbs energy difference as a function of chain length *n*

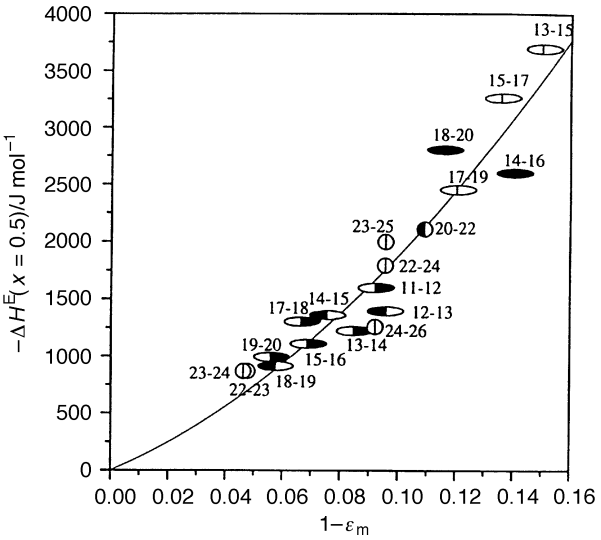

Fig. 7 Representation of excess enthalpy difference as a function of $(1 - \varepsilon_m^i)$

overlap. In Fig. 7 the ΔH^E values are plotted against $(1 - \varepsilon_m^i)$. Although ε_m^i has a general nature, in the special case of the alkanes the values of $(1 - \varepsilon_m^i)$ are close to the values of $\Delta n/n$, the difference in chain length divided by the chain length of the smaller. In spite of the uncertainties in the ΔH^E values (owing to the limitations of the experimental procedures), there is a clear relationship between ΔH^E and $(1 - \varepsilon_m^i)$:

$$\Delta H^E = \{-10\,690(1 - \varepsilon_m^i) - 80\,566(1 - \varepsilon_m^i)^2\}\ J\ mol^{-1} \quad (5)$$

Comparing Fig. 7 and 5 one can observe that the scatter of the data points around the curve in Fig. 7 is more pronounced than in Fig. 5. The reduction of the scatter from Fig. 7 to Fig. 5 is more or less a 'cosmetic' effect owing to the fact that the experimental ΔG^E values correspond to temperatures not far from the compensation temperature of 320 K.

One can also observe that the results do not allow a distinction between the two rotator forms RI and RII. For this reason, the following conclusions refer to the combination of RI and RII as the rotator form.

Two relationships emerge from the set of data. (1) The excess Gibbs energy change for the transition from the rotator form to the liquid passes zero at 320 K, for each of the individual binary systems. The family of systems, therefore, is characterized by a common temperature of excess enthalpy–entropy compensation of 320 K. The excess enthalpy difference and the excess entropy difference have negative values. (2) Within the family the absolute value of the excess enthalpy difference, and consequently also that of the excess entropy difference, increases with the relative mismatch between the crystallographic unit cells of the two components of the binary system.

References

1 P. Espeau, PhD thesis, Université Bordeaux I, France, 1995.
2 L. Robles, PhD thesis, Université Bordeaux I, France, 1995.
3 L. Robles, P. Espeau, D. Mondieig, Y. Haget and H. A. J. Oonk, *Thermochim. Acta*, 1996, **274**, 61.
4 L. Robles, D. Mondieig, Y. Haget, M. A. Cuevas-Diarte and X. Alcobe, *Mol. Cryst. Liq. Cryst.*, 1996, **281**, 279.
5 P. Espeau, Y. Haget, M. A. Cuevas-Diarte and H. A. J. Oonk, in *Les Equilibres Entre Phases*, ed. R. Bouaziz and G. Coquerel, Université Rouen, Rouen, 1995, vol. XXI, p. 67.
6 F. Rajabalee, P. Espeau, Y. Haget and M. A. Cuevas-Diarte, in *Les Equilibres Entre Phases*, ed. R. Bouaziz and G. Coquerel, Université Rouen, Rouen, 1995, vol. XXI, p. 294.
7 L. Robles, D. Mondieig, Y. Haget and M. A. Cuevas-Diarte, in *Les Equilibres Entre Phases*, ed. R. Bouaziz and G. Coquerel, Université Rouen, Rouen, 1995, vol. XXI, p. 301.
8 P. Espeau, H. A. J. Oonk, P. Van der Linde, X. Alcobe and Y. Haget, *J. Chim. Phys.*, 1995, **92**, 747.
9 F. Rajabalee, P. Espeau and Y. Haget, *Mol. Cryst. Liq. Cryst.*, 1995, **269**, 165.
10 E. B. Sirota, H. E. King, H. H. Shao and D. M. Singer, *J. Chem. Phys.*, 1995, **99**, 798.
11 D. L. Dorset, *Acta Chim.*, 1993, **130**, 389.
12 R. R. Matheson and P. Smit, *Polymer*, 1985, **26**, 288.
13 S. K. Filatov and E. N. Kotelnikova, *J. Struct. Chem.*, 1993, **34**, 593.
14 M. Dirand, Z. Achour, B. Jouti, A. Sabour and J. C. Gachon, *Mol. Cryst. Liq. Cryst.*, 1996, **275**, 293.
15 A. Hammami and K. Mehrotra, *Fuel*, 1995, **74**, 96.
16 A. R. Gerson and S. C. Nyburg, *Acta Crystallogr., Sect. B*, 1994, **50**, 252.
17 S. P. Srivastava, J. Handoo, K. M. Agrawal and G. C. Joshi, *J. Phys. Solids*, 1993, **54**, 639.
18 M. Maroncelli, H. L. Strauss and R. G. Snyder, *J. Phys. Chem.*, 1985, **89**, 5260.
19 A. Sabour, PhD thesis, Institut National Polytechnique de Lorraine, Université Nancy, France, 1994.
20 P. Espeau, L. Robles, M. A. Cuevas-Diarte, D. Mondieig and Y. Haget, *Mater. Res. Bull.*, 1996, 31, **10**, 1219.
21 M. Hadjieva, St. Kanev and J. Argirov, *Sol. Energy Mater. Sol. Cells*, 1992, **27**, 181.
22 P. Espeau, L. Robles, D. Mondieig, Y. Haget, M. A. Cuevas-Diarte and H. A. J. Oonk, *J. Chim. Phys.*, 1996, **93**, 1217.
23 L. Robles, P. Espeau, D. Mondieig, Y. Haget and M. A. Cuevas-Diarte, *J. Chim. Phys*, in press.
24 R. G. Snyder, M. Maroncelli, S. P. Qi and H. L. Strauss, *Science*, 1981, **241**, 188.
25 E. B. Sirota, H. E. King, D. M. Singer and H. H. J. Shao, *Chem. Phys.*, 1993, **98**, 5809.
26 E. B. Sirota and D. M. Singer, *J. Chem. Phys.*, 1994, **101**, 10873.
27 I. Denicolo, J. Doucet and A. F. Craievich, *J. Chem. Phys.*, 1983, **78**, 1465.
28 G. Ungar and N. J. Masic, *Phys. Chem.*, 1985, **89**, 1036.
29 G. Ungar, *J. Chem. Phys.*, 1983, **87**, 689.
30 A. Collet, I. Denicolo and A. F. Craievich, *J. Chem. Phys.*, 1981, **75**, 10.
31 R. D. Heyding, R. E. Russel, T. L. Varty and D. St-Cyr, *Powder Diffr.*, 1990, **5**, 93.
32 S. R. Craig, G. P. Hastie, K. J. Roberts and J. N. Sherwood, *J. Mater. Chem.*, 1994, **4**, 977.
33 M. H. G. Jacobs and H. A. J. Oonk, LIQFIT, a computer program for the thermodynamic assessment of vaporus, liquidus, solidus curves in TX phase diagrams (version 1.2), Utrecht University, 1989.
34 H. A. J. Oonk, *Phase Theory: the Thermodynamics of Heterogeneous Equilibria*, Elsevier, Amsterdam, 1981.
35 H. M. J. Boots and P. K. De Bokx, *J. Phys. Chem.*, 1989, **93**, 8240.
36 W. J. M. Van der Kemp, PhD thesis, Utrecht University, 1994.
37 Y. Haget, H. A. J. Oonk and M. A. Cuevas-Diarte, in *Les Equilibres Entre Phases*, ed. J. Kaloustian and J. Pastor, Université Marseille, Marseille, 1990, vol. XVI, p. 35.
38 F. Michaud, PhD thesis, Université Bordeaux I, France, 1994.

Paper 7/03255B; *Received* 12*th May*, 1997